

Surface Interaction Matrices for Boundary Integral Analysis of Lossy Transmission Lines

Anirudha Siripuram, *Student Member, IEEE*, and Vikram Jandhyala, *Senior Member, IEEE*

Abstract—A method intended to characterize enclosed computational electromagnetic domains in terms of interaction and response of a defined set of surface excitations is described. The finite-element method is used to compute a matrix relating surface current and tangential field in terms of an appropriate basis set such that a coupled solution with a boundary integral formulation is rendered seamless. The proposed method allows for a decoupled finite-element boundary-integral system through use of a discrete-frequency surface interaction matrix, computed in an alternative way, that is still independent of the properties of the background in which the enclosed region resides. The method is applied to per-unit-length resistance and inductance extraction of a variety of multiconductor lossy transmission lines. The primary advantage the proposed method presents for this particular application is reuse of matrices given recurrence of specific conductor cross sections.

Index Terms—Decoupled, inductance, lossy transmission line, per unit length, skin effect, surface impedance.

I. INTRODUCTION

DEVICE models serve as essential tools in the solution of linear circuit networks. They provide a convenient means of solving large circuit or RF device networks through I - V characterization or definition of ports and subsequent characterization of port interaction using impedance or admittance relationships. Such characterization often satisfies at least two conditions: the simplified model of a given device is independent of the network in which the device will be placed and the method of interaction between the device and the network is well defined and encompasses all necessary or desired interactions. For situations where frequency and device dimension are such that ideal wire approximations are sufficiently accurate or cases where interaction between a device and the network can be exclusively defined by a finite number of modes associated with well-defined ports, the two previously mentioned conditions can be readily satisfied. For general electromagnetic (EM) problems, such definitions or approximations may not be possible.

A common means of solving such EM problems is through use of computational methods such as the finite-element method

(FEM) or the boundary integral method, which involve volume or surface discretization of regions or surfaces where field intensities or surface currents are expanded in finite-support basis functions defined on the discretized elements. Therefore, a framework may exist for developing models similar to those of circuit devices in terms of these basis functions. The primary purpose of this paper is to present a general technique to characterize arbitrary enclosed regions using the FEM and then to incorporate the result into a boundary integral problem resulting in a decoupled finite-element boundary-integral system. The proposed method will be applied to a problem defined by the lossy 2-D wave equation: parameter extraction of lossy transmission lines.

Parameter extraction of lossy transmission lines is a relatively mature area of research that has gained more attention in recent years due to the need for accurate models of high-speed interconnect, on-chip, package, and board devices. Since conductor material cross sections are typically considered homogeneous, surface equivalence may be used with the boundary integral method to compute parameters such as per-unit-length resistance and inductance [1]. However, boundary integral methods using the surface equivalence principle do not provide an obvious means of *a priori* modeling of the conductor regions. Alternatively, a volume-surface integral approach as implemented by Tsuk and Kong [2], Antonini *et al.* [3], and Coperich *et al.* [4] are also effective options. However, the need to accurately model the attenuating field within the conductor can prohibitively increase the size of the dense matrix system that must be solved. Though tractability of solving matrices defined by 2-D systems is not typically an issue given current computing means, efficient use of computing resources when possible is always preferred. Furthermore, neither of the two methods can take full advantage of repeated conductor cross sections. Some of the more recent techniques attempt to address conductor recurrence by parameterizing the conducting volume through surface interaction. This has been done by Coperich *et al.* [5] using a finite-difference method coupled with a boundary integral formulation and by De Zutter *et al.* [6] using a semianalytical surface admittance operator extraction. A generalization of the latter work to scattering for the TM case is presented by Rogier *et al.* [7]. Use of this semianalytical surface admittance operator can be computationally efficient; however, it limits application to homogeneous and rectangle-shaped conductors. The proposed technique is most similar to these techniques in that it involves computing a matrix akin to a surface impedance operator doing so with a volume differential equation method. One advantage of the proposed method, since it makes use of the FEM, is the general applicability to conductor regions of arbitrary shape and

Manuscript received June 28, 2008; revised September 17, 2008. First published January 19, 2009; current version published February 06, 2009. This work was supported in part by the Department of Defense (DoD) under a Science, Mathematics, and Research for Transformation (SMART) Fellowship.

The authors are with the Applied Computational Engineering Laboratory, University of Washington, Seattle, WA 98195 USA (e-mail: anirus@u.washington.edu; vj@u.washington.edu).

Color versions of one or more of the figures in this paper are available online at <http://ieeexplore.ieee.org>.

Digital Object Identifier 10.1109/TMTT.2008.2011224

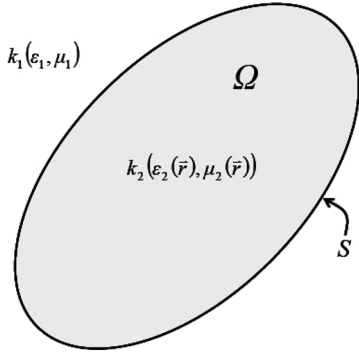


Fig. 1. Bounded inhomogeneous domain residing in an unbounded homogeneous region.

composition. Also, as may become apparent in the ensuing sections, the proposed method does not preclude general extension to 3-D regions.

This paper is organized as follows. Section II provides a motivational reasoning for the proposed technique followed by an exposition on the pertinent finite-element and boundary-integral formulations for the 2-D problems addressed in this paper. In Section III, results are given for a variety of multiconductor transmission-line problems and comparisons to analytical and numerical results are provided. Section IV provides a concluding summary.

II. METHOD AND FORMULATION

What follows is a general motivation, given for a 3-D problem, for the proposed technique followed by the pertinent formulation for the construction and use of an interaction matrix, or impedance matrix in this specific case, in computing per-unit-length parameters of lossy multiconductor transmission lines. First, a homogeneous background transmission-line problem consisting of lossy conductors with arbitrary cross sections is defined. A convenient means of characterizing a given conductor region, using the nodal FEM, is described. The proposed technique yields a matrix relating longitudinally directed surface current to longitudinally directed electric field such that the surface current is expanded in basis functions most commonly used in 2-D boundary integral problems.

A. Surface Equivalence

Though the solution of a two-region problem using surface integral equations is fairly standard, the method is described in order to clarify how the proposed technique relates to the coupled system defined in the surface equivalence problem. Shown in Fig. 1 is a general bounded inhomogeneous region residing in an unbounded homogeneous one. If one assumes for the moment that the bounded region is homogeneous, one may construct equations for exterior and interior problems where total field is assumed to be null in the bounded and unbounded regions respectively. Enforcing the tangential continuity of electric and magnetic fields and thus equating the surface electric

and magnetic currents defined for the interior and exterior problems, the electric field integral equation (EFIE) for the exterior region is given by

$$\hat{n} \times \vec{E}^{\text{inc}}(\vec{r}) = -\vec{M}_s(\vec{r}) + \hat{n} \times \left\{ \nabla \phi_1(\vec{r}) + j\omega\mu_1 \vec{A}_1(\vec{r}) + \nabla \times \vec{F}_1(\vec{r}) \right\} \quad (1)$$

and interior region by [8], [9]

$$\vec{M}_s(\vec{r}) = \hat{n} \times \left\{ \frac{\nabla \nabla \cdot \vec{A}_2(\vec{r}) + k_2^2 \vec{A}_2(\vec{r})}{j\omega\epsilon_2} - \nabla \times \vec{F}_2(\vec{r}) \right\} \quad (2)$$

where

$$\vec{A}_{1,2}(\vec{r}) = \iint_S \vec{J}_s(\vec{r}') G_{1,2}(\vec{r}, \vec{r}') dS(\vec{r}') \quad (3)$$

$$\vec{F}_{1,2}(\vec{r}) = \iint_S \vec{M}_s(\vec{r}') G_{1,2}(\vec{r}, \vec{r}') dS(\vec{r}') \quad (4)$$

$$\phi_{1,2}(\vec{r}) = \iint_S \rho^e(\vec{r}') G_{1,2}(\vec{r}, \vec{r}') dS(\vec{r}') \quad (5)$$

and

$$G_{1,2}(\vec{r}, \vec{r}') = \frac{e^{-jk_{1,2}|\vec{r}-\vec{r}'|}}{4\pi|\vec{r}-\vec{r}'|}. \quad (6)$$

Here, \vec{J}_s , \vec{M}_s , and ρ^e are electric surface current, magnetic surface current, and electric surface charge, respectively. The mixed potential formalism is retained for the exterior region since this is the common form of choice for the application addressed in this paper. The boundary integral method can be used to solve for the coupled system defined by (1) and (2) in a manner similar to that for 3-D scattering [8] or for the 2-D transmission-line case [1]. Of course, (6) only applies for a homogeneous interior region in that the expression for G_2 is not valid for the general case of Fig. 1. One might then ask if the appropriate equation, wave equation in this case, was satisfied in the interior region while concurrently satisfying the null exterior field assumption of (2), could a general relationship between magnetic and electric surface currents for arbitrary interior regions be defined?

It should be apparent that (2) provides a relationship between \vec{J}_s and \vec{M}_s that does not explicitly depend on the properties of the exterior medium. Therefore, if a unique relationship between \vec{J}_s and \vec{M}_s can be arrived at from the interior problem under the null exterior field assumption, then the necessary surface parameterization should be possible. If the interior region is lossy, then the field radiated by any source in the interior region, given that either the tangential electric or magnetic field is prescribed on the boundary, is unique. Therefore, if one enforces

a zero tangential magnetic field on the boundary, the field radiated by an electric current dipole infinitesimally close to and approaching the boundary from the interior region will be unique. Since this boundary is impenetrable, the field in the exterior region will still be null satisfying a supposition of (2). Therefore, one may arrive at a unique relationship between surface current density and tangential electric field by successively testing the entire boundary with current excitations and observing the resulting tangential electric field on the boundary. Alternatively, one could enforce a perfect electric conductor (PEC) boundary condition and test with magnetic current dipoles to arrive at the inverse relationship.

Once such a relationship is known, it may be used in (1) to solve the coupled problem. The given exposition may be an obvious application of the surface equivalence principle and the uniqueness theorem, but the question that the authors hope to answer is whether the interior problem can be set up using the FEM and yield an interaction matrix that can be used in a boundary integral system similar to the one defined by (1). In this way, the enclosed region need not be homogeneous. Such *a priori* modeling can also take advantage of any repeated occurrence of a given bounded region within the computational domain. What follows is one means of achieving this objective for 2-D transmission-line problems.

B. Interior Region—FEM

The proposed application is per-unit-length resistance and inductance extraction of finite-conductivity multiconductor transmission lines. Therefore, the EM problem will be assumed to be TM_z . In this case, the bounded region Ω of Fig. 1 would be invariant in the z -direction and circumscribed by contour Γ . The relationship between z -directed volume current and z -directed electric field is given by the lossy inhomogeneous wave equation [10]

$$\left(\frac{\partial}{\partial x} \mu^{-1}(\boldsymbol{\rho}) \frac{\partial}{\partial x} + \frac{\partial}{\partial y} \mu^{-1}(\boldsymbol{\rho}) \frac{\partial}{\partial y} \right) E_z(\boldsymbol{\rho}) - j\omega\sigma(\boldsymbol{\rho})E_z(\boldsymbol{\rho}) + \omega^2\epsilon(\boldsymbol{\rho})E_z(\boldsymbol{\rho}) = j\omega J_z^v(\boldsymbol{\rho}). \quad (7)$$

The field solution will be subject to the imposed boundary condition, which, as described in Section II-A, will be enforced so that the tangential magnetic field is 0. Since $H_{\text{tan}} \propto (\partial E_z / \partial n)$, the desired boundary condition is $(\partial E_z / \partial n) = 0$.

One may use the standard nodal FEM [10] to readily arrive at a matrix system given by $[K]\{e_z\} = \{j_z^v\}$ where the elemental $[K^e]$ is given by

$$K_{ij}^e = - \iint_{\Omega^e} \frac{1}{\mu^e} \left[\frac{\partial N_i^e}{\partial x} \frac{\partial N_j^e}{\partial x} + \frac{\partial N_i^e}{\partial y} \frac{\partial N_j^e}{\partial y} \right] dx dy + \iint_{\Omega^e} [-j\omega\sigma^e N_i^e N_j^e + \omega^2\epsilon^e N_i^e N_j^e] dx dy \quad (8)$$

and μ , ϵ , and σ are assumed to be constant within each element Ω^e . Here, it will be assumed that N_x^e are linear interpolatory basis functions. Surface current, expanded in pulse basis

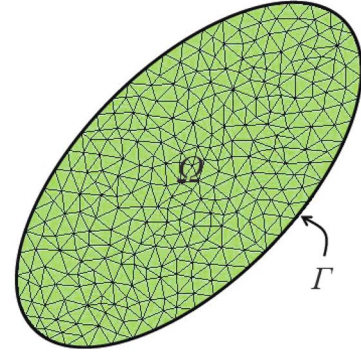


Fig. 2. Example triangular mesh of bounded domain.

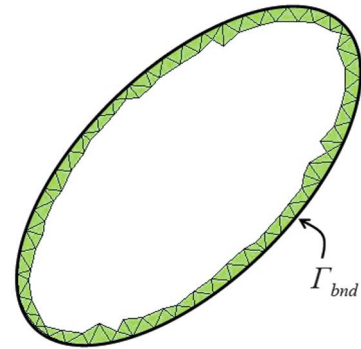


Fig. 3. Example triangular mesh of augmented domain.

function P_s^x , may be introduced as an auxiliary unknown in the same way as done in the standard finite-element boundary-integral method [10] so that

$$[C \quad K] \begin{Bmatrix} j_z^s \\ e_z \end{Bmatrix} = \{0\} \quad (9)$$

where the elemental C_{ij}^s is given by

$$C_{ij}^s = j\omega \int_{\Gamma_s} P_j^s N_i^s d\Gamma. \quad (10)$$

Here, $[C]$ is an $n \times m$ matrix where m is the number of edges on the boundary. The edge-associated N_x^s basis functions are chosen to be of linear order to coincide with the linear N_x^e . The purpose of the remaining portion of this section is to arrive at m additional equations that ensure the homogeneous Neumann boundary condition for electric field, $(\partial E_z / \partial n) = 0$, is satisfied on Γ . This is achieved by conveniently augmenting the original interior domain and providing an additional relationship for $\{j_z^s e_z\}^T$.

It will be assumed that the domain Ω is discretized with triangular elements, as shown in Fig. 2. From this mesh itself, one may construct an additional mesh comprised of a layer or layers of elements that line the boundary, as shown in Fig. 3. This additional meshed region will be referred to as the augmented region. The material parameters of the augmented region are assumed to be identical to those of the corresponding region in the original domain. It should be apparent that every unknown in the augmented domain will have a corresponding unknown in the original domain. Just as was done in (9), a matrix system that

defines surface current can be constructed for the augmented region and is given by

$$[C_{\text{aug}} \quad K_{\text{aug}}] \begin{Bmatrix} j_{z,\text{aug}}^s \\ e_{z,\text{aug}} \end{Bmatrix} = \{0\} \quad (11)$$

where $[K_{\text{aug}}]$ is an $n' \times n'$ matrix with n' being the number of nodal unknowns associated with the augmented domain and $[C_{\text{aug}}]$ an $n' \times m$ matrix where m is still the number of boundary edges on Γ . Assume the electric field unknowns have been ordered such that $\{e_{z,\text{aug}}\} = \{e_{z,\text{aug}}^{\text{bnd}} \ e_{z,\text{aug}}^{\text{int}}\}^T$ where $e_{z,\text{aug}}^{\text{bnd}}$ represent only the unknowns associated with basis functions having support on the boundary Γ_{bnd} and $e_{z,\text{aug}}^{\text{int}}$ represents all other unknowns associated with the augmented domain. The implicit assumption here is that $\{e_{z,\text{aug}}^{\text{int}}\}$ is not a null vector. The matrix relationship given in (11) can be modified such that $e_{z,\text{aug}}^{\text{bnd}}$ is also seen in the right-hand side (RHS). The modified system is given by

$$[C'_{\text{aug}} \quad K'_{\text{aug}}] \begin{Bmatrix} j_{z,\text{aug}}^s \\ e_{z,\text{aug}}^{\text{bnd}} \\ e_{z,\text{aug}}^{\text{int}} \\ e_{z,\text{aug}} \end{Bmatrix} = \begin{Bmatrix} e_{z,\text{aug}}^{\text{bnd}} \\ 0 \end{Bmatrix}. \quad (12)$$

One can readily modify this expression to express an averaged electric field over a boundary segment rather than a value evaluated at a boundary node by averaging the two node electric field values of every boundary edge. Once the rows of $[C'_{\text{aug}} \quad K'_{\text{aug}}]$ are averaged appropriately, m equations can be extracted from the matrix expression of (12) to arrive at an expression given by

$$[C''_{\text{aug}} \quad K''_{\text{aug}}] \begin{Bmatrix} j_{z,\text{aug}}^s \\ e_{z,\text{aug}}^{\text{bnd}} \\ e_{z,\text{aug}}^{\text{int}} \\ e_{z,\text{aug}} \end{Bmatrix} = \{e_z^s\}. \quad (13)$$

Here, the use of linear interpolatory basis functions simplified the relationship between $[C'_{\text{aug}} \quad K'_{\text{aug}}]$ and $[C''_{\text{aug}} \quad K''_{\text{aug}}]$. If more complicated basis sets are used (e.g., higher order, hierarchical, etc.), the construction of $[C''_{\text{aug}} \quad K''_{\text{aug}}]$ would simply involve a weighted averaging where the weight is the integration of a given normalized basis function over the segment.

After enforcing the condition that all unknowns defined for the augmented domain are equal to their respective corresponding values in the original domain and subsequently that $j_z^s = -j_{z,\text{aug}}^s$, it should be apparent that the z -directed electric field will be symmetric about the $\Gamma - \Gamma_{\text{bnd}}$ interface. Therefore, the homogeneous Neumann boundary condition on Γ (i.e., the symmetric boundary condition) will be satisfied for electric field. Combining (9) and (13) yields

$$\begin{bmatrix} C''_{\text{aug}} & KO''_{\text{aug}} \\ -C & K \end{bmatrix} \begin{Bmatrix} j_z^s \\ e_z^{\text{bnd}} \\ e_z^{\text{int}} \\ e_z^{\text{thr}} \end{Bmatrix} = \begin{Bmatrix} e_z^s \\ 0 \end{Bmatrix} \quad (14)$$

where $[KO''_{\text{aug}}] = [K''_{\text{aug}} \ 0]$ since the equations extracted from (13) will only be dependent on e_z^{bnd} and e_z^{int} . Here, e_z^{thr} represents all unknowns associated with the original domain that do not have corresponding values in the augmented domain. One may readily verify that $[C''_{\text{aug}}]$ is a sparse $m \times m$ matrix, $[KO''_{\text{aug}}]$ is a sparse $m \times n$ matrix, $[C]$ is a sparse $n \times m$ matrix, and $[K]$

is a symmetric sparse $n \times n$ matrix. In the Schur complement form, (14) may be written

$$([C''_{\text{aug}}] + [KO''_{\text{aug}}] [K^{-1}] [C]) \{j_z^s\} = \{e_z^s\} \quad (15)$$

which is the desired relationship since it relates surface current to electric field where surface current is expanded in pulse basis functions. Though the proposed technique does not restrict the definition of sources within the bounded domain, the enclosed region(s) here will be assumed passive. This assumption does pose one limitation, which will be discussed in Section II-C, regarding the proposed application.

Since (15) describes a system where the null field is enforced for the region exterior to Ω and that the expression is independent of the properties of that region, then the suppositions of the two-region surface equivalence problem have been met. Furthermore, since the inhomogeneous scalar wave equation is satisfied in Ω , the interior region need not be homogeneous. The matrix given in (15) is similar to the global surface impedance (GSI) matrix proposed by Coperich *et al.* [5]. However, the mapping between the volume- and surface-based methods is seamless in the proposed technique in that the impedance matrix is computed in way that it can be used directly with a boundary integral system matrix, as will be shown. The use of the FEM for the interior problem as opposed to a finite-difference-based method enhances the ability to readily resolve unstructured features and inhomogeneities. A motivational reasoning explaining why the homogeneous Neumann boundary condition is the necessary boundary condition for the interior problem has also been given here.

For convenience,

$$[Z_{\text{int}}] = [C''_{\text{aug}}] + [KO''_{\text{aug}}] [K^{-1}] [C] \quad (16)$$

is defined and may be computed efficiently in a number of ways, but the method employed here makes use of LU decomposition of $[K]$ followed by m solutions of $[K]\{x\} = \{y\}$ where $\{y\}$ are each of the columns of $[C]$. This method can take advantage of the facts that $[K]$ is sparse symmetric, n is typically much larger than m , and $[KO''_{\text{aug}}]$ has many null columns.

C. Exterior Region Solution—Boundary Integral

Under the TM_z assumption, standard EFIE for the homogeneous unbounded exterior problem of (1) simplifies to [9]

$$E_z^{\text{inc}}(\boldsymbol{\rho}) = E_z(\boldsymbol{\rho}) + \frac{\partial \phi(\boldsymbol{\rho})}{\partial z} + j\omega\mu_1 A_z(\boldsymbol{\rho}) + \left\{ \frac{\partial F_y}{\partial x} - \frac{\partial F_x}{\partial y} \right\} \quad (17)$$

where $\boldsymbol{\rho} \in \Gamma$ and a Green's function given by

$$G_1(\boldsymbol{\rho}, \boldsymbol{\rho}') = -\frac{j}{4} H_0^{(2)}(k_1 |\boldsymbol{\rho} - \boldsymbol{\rho}'|). \quad (18)$$

Again, the mixed scalar-vector potential formalism has been retained in (17). Though the discussion in this paper will be restricted to homogeneous exterior regions and thus make use of the free-space Green's function, the proposed technique does not require such a restriction. In addition, since the surface model of the interior region is independent of the exterior region material properties, the trace region can be embedded in more than one background medium without any change

in the impedance matrix. Since the electrical dimension of the transmission-line traces will typically be small and the background region lossless, the static 2-D Green's function $-(1/2\pi) \ln(|\boldsymbol{\rho} - \boldsymbol{\rho}'|)$ will be used when appropriate.

In per-unit-length extraction problems, (17) is typically driven through the electric potential derivative term $\partial\phi/\partial z$ and so, merely for the sake of a consistent notation, the incident field E_z^{inc} is assumed zero. After discretizing the contour Γ and expanding surface current density in pulse basis functions, the matrix form of the given expression can be constructed as done with standard boundary-integral problems [9]–[11]. The resulting system matrix follows as

$$[Z] \{j_z^s\} + ([I] + [F]) \{e_z^s\} = - \left\{ \frac{\partial\phi}{\partial z} \right\} \quad (19)$$

where $[I]$ is the identity matrix and $[F]$ is the matrix defined by the derivative of G_1 [1]. If one assumes a known surface impedance matrix $[Z_{\text{int}}]$ relating $\{j_z^s\}$ to $\{e_z^s\}$, then (19) may be written

$$([Z] + ([I] + [F])[Z_{\text{int}}]) \{j_z^s\} = - \left\{ \frac{\partial\phi}{\partial z} \right\}. \quad (20)$$

Though the electric vector potential term is sometimes retained [1], its effect is often neglected in per-unit-length extraction [2], [3], [5], [6], [12]. In this case, the defining equation for the boundary integral system is given by

$$-\frac{\partial\phi(\boldsymbol{\rho})}{\partial z} = E_z(\boldsymbol{\rho}) + j\omega\mu_1 A_z(\boldsymbol{\rho}) \quad (21)$$

and it follows that

$$([Z] + [Z_{\text{int}}]) \{j_z^s\} = - \left\{ \frac{\partial\phi}{\partial z} \right\}. \quad (22)$$

D. Extracting Per-Unit-Length Resistance and Inductance

If one assumes a general multiconductor transmission line consisting of p_c conductors—the first p_{sig} of which are signal lines with the remaining conductor(s) serving as reference—and that $[Z_{\text{int}}^p]$ and $j_z^{s,p}$ refer to the interior interaction matrix and the surface current unknowns of the p th conductor, respectively, then the multiconductor interior–exterior system is described by

$$[Z_{\text{tot}}] \begin{Bmatrix} j_z^{s,1} \\ j_z^{s,2} \\ \vdots \\ j_z^{s,p_c} \end{Bmatrix} = - \left\{ \frac{\partial\phi}{\partial z} \right\} \quad (23)$$

where

$$[Z_{\text{tot}}] = \begin{bmatrix} Z_{11} & Z_{12} & \vdots \\ Z_{21} & \ddots & \vdots \\ \dots & \dots & Z_{p_c p_c} \end{bmatrix} + \begin{bmatrix} Z_{\text{int}}^1 & 0 & \vdots \\ 0 & \ddots & \vdots \\ \dots & \dots & Z_{\text{int}}^{p_c} \end{bmatrix}. \quad (24)$$

A common assumption for combined volume-surface integral methods for per-unit-length parameter extraction is that the potential is constant over an entire conductor cross section [2]. With this condition and the condition that a return path

for current transmitted through a given signal line is provided through the reference conductor(s), one can arrive at all self resistances and self inductances. Unfortunately, satisfying the first condition will not be possible with the proposed technique since applying an excitation $\partial\phi/\partial z$ from the interior of the conductor cross section, as mentioned earlier, is not possible. Subsequently, only qualitative comparison to results achieved using a volume-surface integral approach is possible. Validation of the proposed technique will rely more on comparison to analytical results, to results of surface current techniques, and to known asymptotic behavior.

Using the two conditions mentioned, $p_{\text{sig}} + 1$ additional equations and unknowns can be introduced. The equations for current are $\sum_{q=1}^{s_i} j_z^{s,i(q)} i^{(q)} = c_i$ for each $i = 1, 2, \dots, p_{\text{sig}}$ and $\sum_{p=p_{\text{sig}}+1}^{p_c} \sum_{q=1}^{s_p} j_z^{s,p(q)} p^{(q)} = c_{\text{ref}}$. Here, l is the length of a boundary segment, exponent $p(q)$ denotes the q th boundary segment of the p th conductor, and s_p is the number of boundary segments for the p th conductor. The additional unknowns $(\partial\phi/\partial z)|_{p=i}$ for $i = 1, 2, \dots, p_{\text{sig}}$ and $(\partial\phi/\partial z)|_{p=p_{\text{sig}}+1}$ represent the constant boundary potential per-unit-length on each signal conductor and all reference conductors, respectively. With the additional constraints and unknowns, the driven system is

$$\begin{bmatrix} Z_{\text{tot}} & V \\ L & \mathbf{0} \end{bmatrix} \begin{Bmatrix} j_z^s \\ \frac{\partial\phi}{\partial z}|_{p=1} \\ \frac{\partial\phi}{\partial z}|_{p=2} \\ \vdots \\ \frac{\partial\phi}{\partial z}|_{p=p_{\text{sig}}+1} \end{Bmatrix} = \begin{Bmatrix} \bar{0} \\ \bar{c} \end{Bmatrix} \quad (25)$$

with $\bar{c} = \{c_1, c_2, \dots, c_{p_{\text{sig}}+1}\}^T$. Matrix $[V]$ is $m \times p_{\text{sig}} + 1$ where the i th column has ones for all edge indices associated with conductor i and zeros elsewhere with the exception of the last column that has ones for edge indices associated with all reference conductors and zeros elsewhere. Similarly, $[L]$ is $p_{\text{sig}} + 1 \times m$ where the i th row contains the edge lengths, at the appropriate indices, associated with the i th conductor and zeros elsewhere with the exception of the last row that contains only the edge lengths of all reference conductors. The self and mutual resistances and inductances are computed in the same way as done by Tsuk *et al.* [2] who employ integration of surface quantities over line integrals rather than integration of i th circuit flux [13]. Since the proposed method solves for surface unknowns, it is possible to compute the total per-unit-length reactive power directly by summing the individual contributions of reactive power from the boundary edges of each conductor. If reactive power $S^{p(q)}$ per-unit-length for the q th boundary edge of the p th conductor is given by

$$S^{p(q)} = \frac{1}{2} \left(j_z^{s,p(q)} \right)^* p^{(q)} \frac{\partial\phi}{\partial z} \Big|_p \quad (26)$$

then the total per-unit-length reactive power follows as

$$S = \sum_{p=1}^{p_c} \sum_{q=1}^{s_p} S^{p(q)}. \quad (27)$$

TABLE I
COMPUTED PER-UNIT-LENGTH RESISTANCE IN $m\Omega/m$ OVER FREQUENCY
FOR A SQUARE 4.62-mm COPPER ($\sigma = 5.72 \times 10^7$ S/m)
CONDUCTOR FOR VARIOUS SURFACE AND EDGE MESH DENSITIES
(SURFACE ELEMENTS, BOUNDARY EDGES)

frequency (Hz)	{950, 72}	{2300, 140}	{4326, 280}	{8946, 556}
10^2	0.81949	0.81950	0.81950	0.81950
10^3	0.86031	0.86025	0.86024	0.86024
10^4	1.8730	1.8652	1.8639	1.8636
10^5	5.7606	5.5510	5.5132	5.5013
10^6	18.346	18.818	17.790	17.428

All self terms may be computed by driving a signal current, assumed to be 1 A, through conductor i allowing it to return through the reference conductors which implies solving (25) with $c_i = 1$ and $c_{\text{ref}} = -1$ (zero assumed otherwise). If the relationship between reactive power and impedance is given by $S = (1/2)|I|^2\Re\{Z\} + j(1/2)|I|^2\Im\{Z\}$, the per-unit-length resistance and inductance follow as

$$R_{\text{pul},ii} = \Re\{2S\} \quad (28)$$

and

$$L_{\text{pul},ii} = \Im\{2S/\omega\} \quad (29)$$

which will yield the desired self terms assuming the solution of (25) is used in (26) and (27). Reactance is assumed to be inductive in this TM_z scenario since the field solution cannot support transverse electric current. The mutual terms may be arrived at by first driving a signal current, assumed to be 1 A, through conductor i allowing it to return through conductor j so that (25) is solved with $c_i = 1$ and $c_j = -1$ (zero assumed otherwise). Using this solution in (26) and (27), the mutual terms follow as [2]

$$R_{\text{pul},ij} = \frac{1}{2}(R_{ii} + R_{jj} - 2\Re\{S\}) \quad (30)$$

and

$$L_{\text{pul},ij} = \frac{1}{2}(L_{ii} + L_{jj} - 2\Im\{S\}/\omega). \quad (31)$$

III. NUMERICAL RESULTS

A. Single Conductor Interconnect Problem

For the first example, R_{pul} is computed for a single 4.62 mm \times 4.62 mm conductor with $\sigma = 5.72 \times 10^7$ S/m residing in free space. The results for various triangular element and boundary edge densities is given in Table I.

One can observe the convergent behavior of the solution as mesh density is increased. Low-frequency values also agree with the dc resistance of 0.81906 $m\Omega/m$. The results shown in Table I tend to agree with those presented by De Zutter *et al.* [12]. Their surface admittance operator method is similar to the method described in this paper in that a model of the conductor region is computed *a priori* and used in a boundary integral

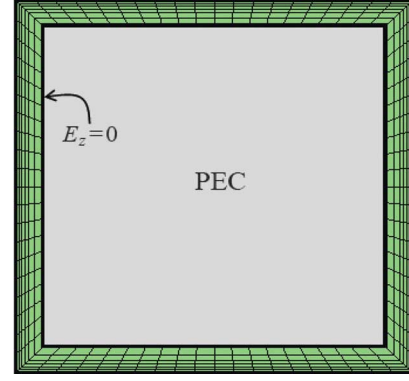


Fig. 4. Example quadrilateral mesh that better accommodates exponentially decaying fields near exterior boundaries.

TABLE II
COMPUTED PER-UNIT-LENGTH RESISTANCE IN $m\Omega/m$ AT TRANSITION REGION
FREQUENCIES FOR A SQUARE 4.62-mm COPPER ($\sigma = 5.72 \times 10^7$ S/m)
CONDUCTOR USING QUADRILATERAL MESHES EXTENDING
TO A DEPTH OF $5\delta(f)$

frequency (Hz)	δ (mm)	# of layers	40 edges	80 edges	200 edges	300 edges
10^5	0.2104	20	5.3809	5.5214	5.5070	5.5009
10^6	0.0665	10	15.950	16.589	17.247	17.294

formulation such that the coupled problem is driven through surface excitations. However, their admittance operator does have a dependence on the background medium which indicates an inherent difference in the two formulations. The results also compare qualitatively to those of Tsuk and Kong [2] and Antonini *et al.* [3] though both of these formulations extract parameters using volume current excitations.

At higher frequencies where the skin effect is well developed, triangular meshes may need to be made prohibitively dense near the conductor boundary to accurately model the field decay there. A quadrilateral mesh, as shown in Fig. 4, may be more appropriate due to the approximately exponential decay of field in the direction normal to the boundary. In Fig. 4, the interior of the trace is not meshed since it will be assumed that the field is zero beyond a depth of five times the skin depth δ where $\delta = \sqrt{2/(\omega\mu_0\sigma)}$. In Table II, R_{pul} is given for transition—from volumetric to surface current—frequencies. The results show not only a convergence with increase in mesh density, but also general agreement with the results of Table I.

B. Two-Conductor Problems

For a multiconductor example, a two conductor problem consisting of identical 2 mm \times 2 mm conductors separated by a distance d , as shown in Fig. 5(a), with conductivity $\sigma = 5.6 \times 10^7$ S/m residing in free space is studied. From Fig. 6, the resistance at 100 Hz agrees well with the dc value of 8.9286 $m\Omega/m$. At higher frequencies, the resistance approaches the expected $f^{1/2}$ relationship predicted by Wheeler [14]. Due to the large dynamic range of frequencies, a refined triangular mesh is used for the FEM region for the range 100 Hz–1 MHz and a PEC terminated quadrilateral mesh, resembling that of Fig. 4, is used for the range of 1 MHz–10 GHz. A seamless transition between

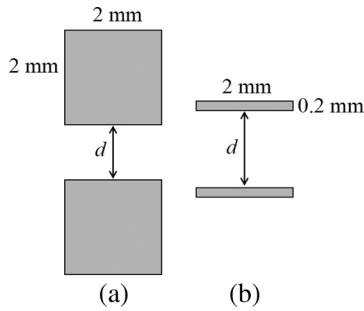


Fig. 5. Conductor configurations for two-conductor simulations.

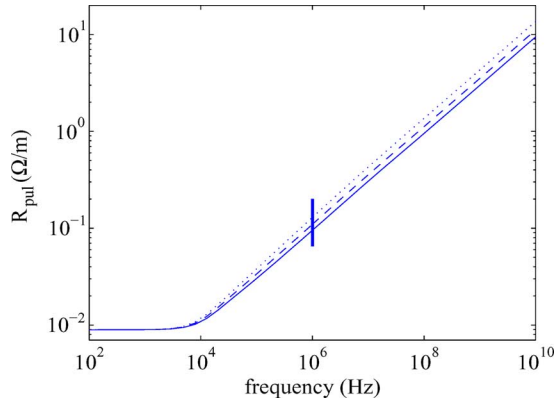


Fig. 6. Computed per-unit-length resistance R_{pul} values of a two-conductor system with $2\text{ mm} \times 2\text{ mm}$ conductor dimensions and vertical separation distances of $d = 2\text{ mm}$ (solid line), $d = 1\text{ mm}$ (dashed line), and $d = 0.5\text{ mm}$ (dotted line).

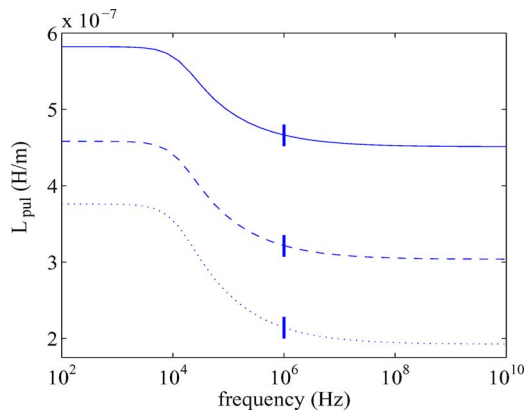


Fig. 7. Computed per-unit-length inductance L_{pul} values of a two-conductor system with $2\text{ mm} \times 2\text{ mm}$ conductor dimensions and vertical separation distances of $d = 2\text{ mm}$ (solid line), $d = 1\text{ mm}$ (dashed line), and $d = 0.5\text{ mm}$ (dotted line).

the two solutions can be observed for both resistance and inductance, as seen in Figs. 6 and 7, respectively (transition denoted by divider in these figures). The inductance for separation distances of 2, 1, and 0.5 mm approach computed, using an exclusively boundary integral method, PEC inductances of 451.16, 303.58, and 192.36 nH/m, respectively.

In a similar example, as shown in Fig. 5(b), the square cross-section conductors are replaced by $0.2\text{ mm} \times 2\text{ mm}$ conductors. Again, the resulting resistances (Fig. 8) reveal the $f^{1/2}$ relationship at higher frequencies and are in agreement with the dc value

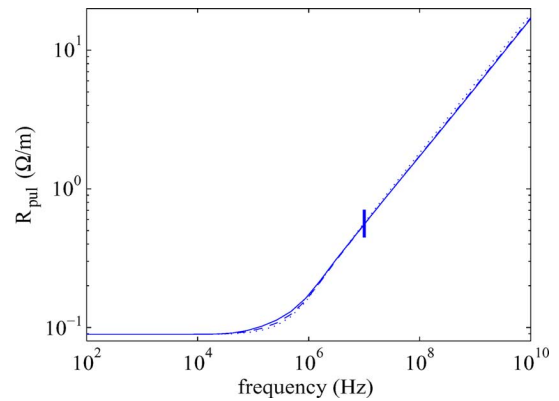


Fig. 8. Computed per-unit-length resistance R_{pul} values of a two-conductor system with $0.2\text{ mm} \times 2\text{ mm}$ conductor dimensions and vertical separation distances of $d = 2\text{ mm}$ (solid line), $d = 1\text{ mm}$ (dashed line), and $d = 0.5\text{ mm}$ (dotted line).

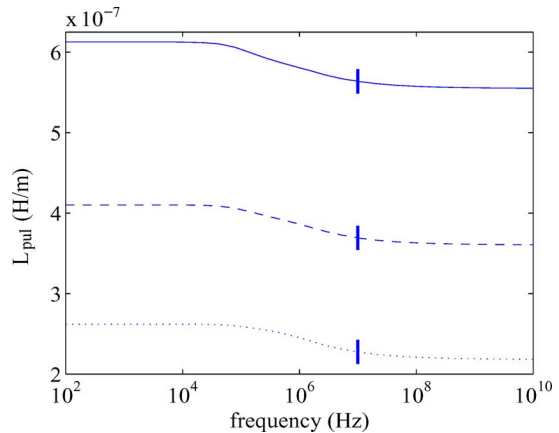


Fig. 9. Computed per-unit-length inductance L_{pul} values of a two-conductor system with $0.2\text{ mm} \times 2\text{ mm}$ conductor dimensions and vertical separation distances of $d = 2\text{ mm}$ (solid line), $d = 1\text{ mm}$ (dashed line), and $d = 0.5\text{ mm}$ (dotted line).

of $89.285\text{ m}\Omega/\text{m}$. Inductances, shown in Fig. 9, at separation distances of 2, 1, and 0.5 mm approach computed PEC inductances of 554.93, 360.30, and 218.01 nH/m, respectively. Comparing the given results with those of De Zutter *et al.* reveals a close agreement for both resistance and inductance though low-frequency inductances appear to somewhat underestimate their values [12]. A qualitative agreement with the results of Djordjevic *et al.* can be observed [1]. However, a direct comparison to their results may not be possible since the excitation method employed here differs significantly from theirs.

Analytical expressions for transmission-line parameters of most multiconductor lines cannot be readily derived. However, Schelkunoff's rigorous derivation of transmission-line parameters of the lowest order mode for coaxial configurations provides a convenient analytical comparison to the numerical results of the proposed method [15]. Analytical expressions for the per-unit-length inductance and resistance of coaxial lines constructed with a single type of conductor residing in a homogeneous background medium (as shown in Fig. 10) have been given by Tesche [16].

Table III compares data computed using triangular meshes for both the inner and outer conductors for a specific configuration

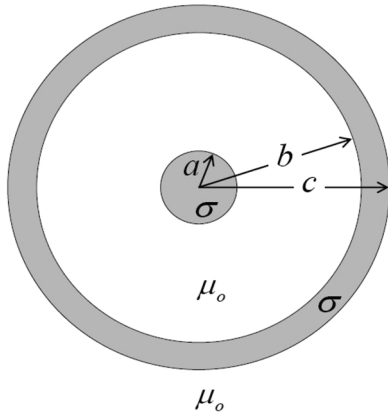


Fig. 10. Coaxial transmission-line configuration.

TABLE III
COMPARISON OF NUMERICAL AND ANALYTICAL T-LINE PARAMETERS FOR
COAXIAL LINE WITH $a = 2.5$ mm, $b = 9.345$ mm,
 $c = 9.945$ mm, AND $\sigma = 5.76 \times 10^7$ S/m

frequency (Hz)	R_{pul} m Ω /m	R_{pul}^a m Ω /m	L_{pul} nH/m	L_{pul}^a nH/m
1×10^2	1.3627	1.3620	316.08	317.98
5×10^2	1.3715	1.3710	315.83	317.72
1×10^3	1.3983	1.3980	315.09	316.97
5×10^3	1.8888	1.8923	302.23	304.07
1×10^4	2.3995	2.4158	292.19	294.02
5×10^4	4.6435	4.8904	277.66	278.73

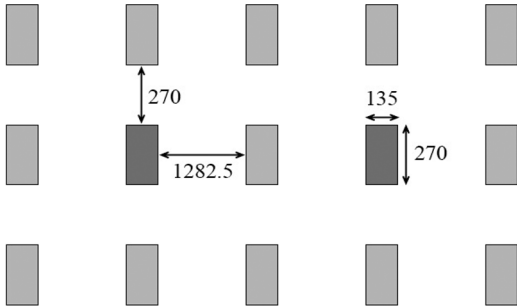


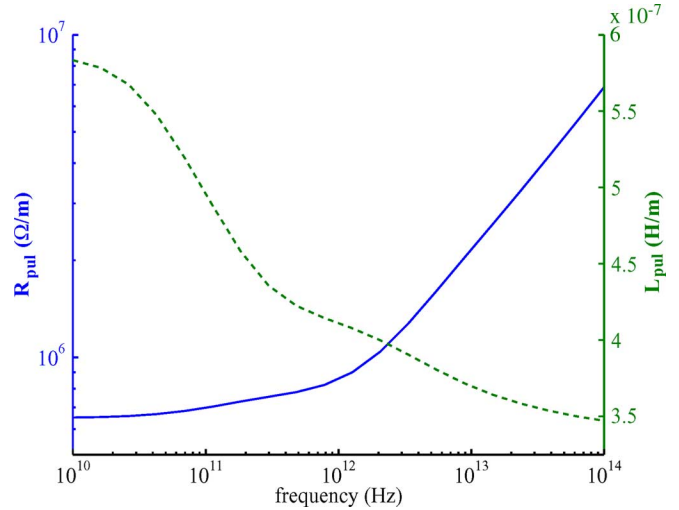
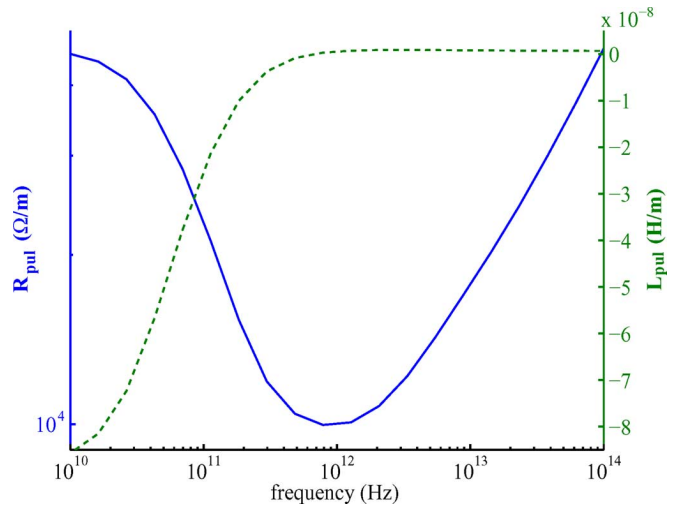
Fig. 11. Multiconductor configuration with two signal lines.

used by Tesche [16] where the average triangle dimension is roughly 1/3 the estimated skin depth at 50 kHz.

C. Multiconductor Problem

As a final example, results for a multiconductor example taken from a paper by De Zutter *et al.* are given [12]. The multiconductor coupled signal line configuration is shown in Fig. 11. In this example, the two darker shaded conductors are the signal lines while the remaining conductors are the reference lines. Conductor conductivity is assumed to be 4.54545×10^7 S/m with a free-space background permeability. All lengths are given in nanometers.

The low-frequency (at 1 MHz) self and mutual per-unit-length resistances and inductances were computed to be $R_{11} = R_{22} = 6.4999 \times 10^5 \Omega/m$, $R_{12} = R_{21} = 4.6428 \times 10^4 \Omega/m$, $L_{11} = L_{22} = 587.58$ nH/m, and $L_{12} = L_{21} = -88.500$ nH/m. The resistance values agree closely with the analytical values

Fig. 12. Self resistance $R_{pul,11}$ (solid line) and self inductance $L_{pul,11}$ (dashed line) for 15-conductor configuration of Fig. 11.Fig. 13. Mutual resistance $R_{pul,12}$ (solid line) and inductance $L_{pul,12}$ (dashed line) for 15-conductor configuration of Fig. 11.

($R_{11} = 6.5000 \times 10^5 \Omega/m$ and $R_{12} = 4.6427 \times 10^4 \Omega/m$) presented by De Zutter *et al.*, while the inductance values somewhat underestimate their computed values ($L_{11} = 599.0$ nH/m and $L_{12} = -89.61$ nH/m) [12]. Computed self and mutual inductances for PECs in the configuration of Fig. 11 have been computed to be 336.90 and 0.59519 nH/m, respectively. One may observe from Figs. 12 and 13 that these values are approached as frequency is increased (347.13 and 0.65732 nH/m at 10^{14} Hz where $\delta = 7.4650$ nm).

IV. CONCLUSIONS

A method intended to develop surface interaction models of enclosed regions of EM problems has been described. The technique makes use of the FEM and yields an interaction matrix that characterizes the relationship between surface current and tangential field on the bounding surface such that current is expanded in a basis set appropriate for standard boundary integral techniques. The interaction matrix is used with a

boundary integral system matrix to solve a decoupled finite-element boundary-integral system. The proposed method has been applied to a 2-D application, per-unit-length resistance, and inductance extraction of lossy transmission lines, yielding accurate results for a variety of single and multiconductor configurations having conductor cross sections of arbitrary shape.

ACKNOWLEDGMENT

The authors would like to thank Dr. J. Meloling and Dr. J. Rockway of the Space and Naval Warfare Systems Center at San Diego (SPAWARSYSCEN-SD), San Diego, CA, for their support.

REFERENCES

- [1] A. Djordjevic, T. Sarkar, and S. Rao, "Analysis of finite conductivity cylindrical conductors excited by axially-independent TM electromagnetic field," *IEEE Trans. Microw. Theory Tech.*, vol. MTT-33, no. 10, pp. 960–966, Oct. 1985.
- [2] M. Tsuk and J. Kong, "A hybrid method for the calculation of the resistance and inductance of transmission lines with arbitrary cross sections," *IEEE Trans. Microw. Theory Tech.*, vol. 39, no. 8, pp. 1338–1346, Aug. 1991.
- [3] G. Antonini, A. Orlandi, and C. Paul, "Internal impedance of conductors of rectangular cross section," *IEEE Trans. Microw. Theory Tech.*, vol. 47, no. 7, pp. 979–985, Jul. 1999.
- [4] K. Coperich, J. Morse, V. Okhmatovski, A. Cangellaris, and A. Ruehli, "Systematic development of transmission-line models for interconnects with frequency-dependent losses," *IEEE Trans. Microw. Theory Tech.*, vol. 49, no. 10, pp. 1677–1685, Oct. 2001.
- [5] K. Coperich, A. Ruehli, and A. Cangellaris, "Enhanced skin effect for partial-element equivalent-circuit (PEEC) models," *IEEE Trans. Microw. Theory Tech.*, vol. 48, no. 9, pp. 1435–1442, Sep. 2000.
- [6] D. De Zutter and L. Knockaert, "Skin effect modeling based on a differential surface admittance operator," *IEEE Trans. Microw. Theory Tech.*, vol. 53, no. 8, pp. 2526–2538, Aug. 2005.
- [7] H. Rogier, D. De Zutter, and L. Knockaert, "Two-dimensional transverse magnetic scattering using an exact surface admittance operator," *Radio Sci.* vol. 42, no. 3201, 2007, DOI 10.1029/2006RS003516.
- [8] K. Umashankar, A. Taflov, and S. Rao, "Electromagnetic scattering by arbitrary shaped three-dimensional homogeneous lossy dielectric objects," *IEEE Trans. Antennas Propag.*, vol. AP-34, no. 6, pp. 758–766, Jun. 1986.
- [9] A. F. Peterson, S. L. Ray, and R. Mittra, *Computational Methods for Electromagnetics*, 1st ed. Piscataway, NJ: IEEE Press, 1998.
- [10] J. Jin, *The Finite Element Method in Electromagnetics*, 2nd ed. New York: Wiley, 2002.
- [11] R. Harrington, *Field Computation by Moment Methods*, 1st ed. Melbourne, FL: Krieger, 1968.
- [12] D. De Zutter, H. Rogier, L. Knockaert, and J. Sercu, "Surface current modelling of the skin effect for on-chip interconnections," *IEEE Trans. Adv. Packag.*, vol. 30, no. 2, pp. 342–349, May 2007.
- [13] C. Paul, *Analysis of Multiconductor Transmission Lines*, 1st ed. New York: Wiley, 1994.
- [14] H. Wheeler, "Formulas for the skin effect," *Proc. IRE*, vol. 30, no. 9, pp. 412–424, Sep. 1942.
- [15] S. Schelkunoff, "The electromagnetic theory of coaxial transmission lines and cylindrical shields," *Bell Syst. Tech. J.*, vol. 13, no. 4, pp. 532–579, 1934.
- [16] F. Tesche, "A simple model for the line parameters of a lossy coaxial cable filled with a nondispersive dielectric," *IEEE Trans. Electromagn. Compat.*, vol. 49, no. 1, pp. 12–17, Feb. 2007.



Anirudha Siripuram (S'08) received the B.S. degree in electrical engineering from the Virginia Polytechnic Institute and State University, Blacksburg, VA, in 2002, the M.S. degree in electrical engineering from the University of Illinois at Urbana-Champaign, in 2004, and is currently working toward the Ph.D. degree in electrical engineering at the University of Washington, Seattle.

From 2002 to 2004, he was a Research Assistant with the Center for Computational Electromagnetics Laboratory (CCEML), University of Illinois at Urbana-Champaign. From 2004 to 2006, he was an Applied Research Engineer with the Space and Naval Warfare Systems Center at San Diego (SPAWARSYSCEN-SD), San Diego, CA. Since 2006, he has been with the Applied Computational Engineering (ACE) Laboratory, University of Washington.



Vikram Jandhyala (S'96–M'00–SM'03) received the B.Tech. degree in electrical engineering from the Indian Institute of Technology (IIT), Delhi, India, in 1993, and the M.S. and Ph.D. degrees from the University of Illinois at Urbana-Champaign, in 1995 and 1998, respectively.

From 1998 to 2000, he was a Research and Development Engineer with the Ansoft Corporation, Pittsburgh, PA. From 2000 to 2005, he was an Assistant Professor with the Electrical Engineering Department, University of Washington, Seattle. He is currently an Associate Professor with the University of Washington, where he directs the Applied Computational Engineering (ACE) Laboratory. He is currently on partial leave from the University of Washington while serving as founder and CEO of Physware Inc., Seattle, WA. His research interests and projects concern several areas of computational electromagnetics including fast solvers and integral equation formulations in the frequency and time domains, high-speed circuits and devices, coupled multiphysics simulation, novel materials, and propagation.